Endostatin gene therapy delivered by attenuated Salmonella typhimurium in murine tumor models

Article *in* Cancer Gene Therapy · August 2018

DOI: 10.1038/s41417-018-0021-6

CITATIONS
7

READS
105

7 authors, including:

Kang Liang
Southwest Normal University
28 PUBLICATIONS **119** CITATIONS
SEE PROFILE

Pei Li
College of Animal Science and Technology
26 PUBLICATIONS **82** CITATIONS
SEE PROFILE

Yue Han
Zhejiang A&F University
23 PUBLICATIONS **58** CITATIONS
SEE PROFILE

Qingke Kong
Arizona State University
63 PUBLICATIONS **666** CITATIONS
SEE PROFILE

Cancer Gene Therapy
https://doi.org/10.1038/s41417-018-0021-6

ARTICLE

Endostatin gene therapy delivered by attenuated *Salmonella typhimurium* in murine tumor models

Kang Liang[1] · Qing Liu[2] · Pei Li[1] · Yue Han[1] · Xiaoping Bian[2] · Yibo Tang[2] · Qingke Kong[1,2]

Received: 18 January 2018 / Accepted: 6 March 2018

Abstract

Salmonella typhimurium (hereafter *S. typhimurium*), as Gram-negative facultative anaerobic bacteria, are good candidates for cancer therapy and delivering therapeutic antitumor agents. However, it is necessary to reduce the virulence of such bacteria and enhance their tumor-targeting ability, and their immunostimulatory ability to induce tumor cell apoptosis. In this study, we constructed a *S. typhimurium* mutant named S634 harboring *aroA* mutation and additional mutations involved in modifications of lipid A. Upon intraperitoneal infection in mice, the *aroA*-deficient strain S634 showed greatly attenuated virulence and preferential accumulation within tumor tissue. We next investigated the ability of S636, the *asd* mutant derivative of S634, to deliver the anti-angiogenic agent "endostatin" (S636/pES) and to inhibit tumor growth in mouse CT26 colon carcinoma and B16F10 melanoma models. S636/pES-treated tumor-bearing mice showed suppressed tumor growth and prolonged survival, compared to mice treated with either the bacteria carrying empty plasmids or PBS intraperitoneally. Immunohistochemical studies demonstrated that, when tumor-bearing mice were infected with S636/pES, *Salmonella* colonization and endostatin expression were accompanied by the increase of apoptosis level and suppression of tumor angiogenesis within tumor tissues. Our findings showed that endostatin gene therapy delivered by attenuated *S. typhimurium* displays therapeutic antitumor effects in murine tumor models.

Introduction

Conventional tumor therapies including chemotherapy, radiotherapy, and surgery have obvious limitations, such as the toxicity to normal tissues or cells, low tumor-targeting, and the disability of penetrating tumor tissue, and usually resulting in incomplete damage to the tumor [1]. Therefore, it is necessary to explore more effective means for cancer treatments. Early studies have demonstrated that some obligate or facultative anaerobes have natural preference for tumor tissue, such as *Clostridium* [2], *Bifidobacterium* [3], *Escherichia coli* [4], and *Salmonella* [5, 6]. Especially, *Salmonella*, as Gram-negative and facultative anaerobic bacteria, have many potential advantages in tumor therapy. (i) *Salmonella* preferentially accumulate within tumor tissue compared to normal tissues [7], and motile *Salmonella* may disperse into different regions of tumor tissue [8, 9]. (ii) *Salmonella* can attack a variety of tumors, such as colorectal carcinoma, melanoma, breast cancer, and prostate cancer, leading to inhibition of tumor growth through multiple mechanisms [1]. (iii) *Salmonella* can be developed as live attenuated bacterial vectors for delivering tumor therapeutic agents, including cytokines, anti-angiogenic agents, tumor antigens, apoptosis-inducing factors, and small interference RNAs [10]. (iv) *Salmonella* with the immunomodulatory ability can elicit strong adjuvant activities [11, 12], thereby improving therapeutic benefits when combined with other cancer treatments [13, 14].

These authors contributed equally: Kang Liang and Qing Liu.

All applicable international, national, and/or institutional guidelines for the care and use of animals were followed. The animal care protocol was approved by Sichuan Agricultural University. All efforts were made to minimize animal suffering during the experiments.

Electronic supplementary material The online version of this article (https://doi.org/10.1038/s41417-018-0021-6) contains supplementary material, which is available to authorized users.

✉ Qingke Kong
kongqiki@163.com

[1] Institute of Preventive Veterinary Medicine, College of Veterinary Medicine, Sichuan Agricultural University, 611130 Chengdu, China

[2] College of Animal Science and Technology, Southwest University, 400715 Chongqing, China

Published online: 14 May 2018

In the past two decades, therapeutic antitumor effects mediated by recombinant attenuated *Salmonella* have been widely studied in animal models and human clinical trials [15–17]. Notably, considering intrinsically pathogenic properties of *Salmonella*, efficient attenuation of bacterial virulence is the prerequisite for the application of *Salmonella* in preclinical and clinical studies. For example, the well-known *S. typhimurium* strain termed VNP20009 [6] was lipid A-modified (*msbB*$^-$) and auxotrophic (*purI*$^-$), in which the gene *purI* is responsible for the adenine synthesis. The tumor-seeking auxotrophic strain named A1-R, which requires arginine and leucine for growth, has been tested for tumor-targeting and antitumor efficacy on a variety of murine tumor models [18–21]. Besides, since the study of SL7202 by Hoiseth and Stocker [22], the auxotrophic mutation of *aroA*-deficiency has been universally used to attenuate bacterial strains and generally considered safe [23].

Lipopolysaccharide (LPS) present in almost all Gram-negative bacteria is the major component of the outer leaflet of the outer membrane and a well-known inducer of the innate immune responses [24]. It consists of the highly variable O-antigen polysaccharide, a short core oligosaccharide, and the anchor lipid A [25, 26]. Lipid A represents the most conserved portion of LPS. Extracellular lipid A is recognized by TLR4 [27] while cytosolic caspase-11 will sense intracellular lipid A to promote the innate immune response [28–30]. The studies regarding structure-activity relationship of lipid A indicate that factors including the number, length, and symmetry of the fatty acid chains of lipid A govern its immunological activity [31, 32]. Among these factors, the total number of fatty acid chains is the most important one. Previous study indicated that the failure of clinical human trial using VNP20009 may be partially attributable to its generating penta-acylated lipid A, which is an antagonist for TLR4 and caspase-11. S633, the parent strain of S634 used in this study, was a *S. typhimurium* mutant with modifications of bacterial LPS (Δ*pagL7* Δ*pagP8* Δ*lpxR9* Δ*arnT2* Δ*eptA3* Δ*lpxT4*), which harbors hexa-acylated lipid A that has been considered to possess the most potent immunomodulatory activity [31].

It has been widely recognized that angiogenesis, the formation of new capillaries from pre-existing vasculature, is critical for tumor growth and metastasis [33]. Thus, inhibition of angiogenesis inside tumor tissue is another potential direction of cancer treatments. The anti-angiogenic strategy targets stable proliferative endothelial cells in the tumor vasculature rather than genetically unstable tumor cells and thereby reduces the probability of drug-resistance in the case of repeated dosing. Endostatin, a 20-kDa C-terminal fragment of type XVIII collagen, discovered in 1997 [34], is one of the most potential inhibitors of angiogenesis. Endostatin has been shown to bind to a variety of receptors on the surface of endothelial cells [35], blocking the proliferation and migration of endothelial cells [36] and inducing endothelial cell apoptosis on the cellular level [37]. In detail, endostatin competitively inhibits the binding of vascular endothelial growth factor (VEGF) to endothelial cells, blocking VEGF-induced tyrosine phosphorylation of KDR/Flk-1, and thus affecting mitogenic activities of VEGF on endothelial cells [38]. Endostatin competes with fibronectin and proangiogenic ligand to prevent binding to integrin α5β1, thereby disrupting the migration of endothelial cells [39]. Endostatin specifically binds to nucleolin on the cell surface with high affinity and can be internalized and transported into cell nuclei of endothelial cells via nucleolin. In the nuclei, endostatin inhibits the phosphorylation of nucleolin, which is critical for the proliferation of endothelial cells [40]. Animal studies also demonstrated that endostatin could suppress tumor growth by suppressing the neovascularization [41–43]. But unfortunately, phase II studies of recombinant endostatin in the United States showed significantly low anti-angiogenic potency [44, 45]. In 2005, Endostar, a novel recombinant human endostatin purified from *Escherichia coli* with an additional His-tag structure, was approved by the State Food and Drug Administration of China (SFDA) for the treatment of non-small cell lung cancer [46]. In order to improve therapeutic antitumor efficacy of endostatin, different delivery vehicles were used, which include virus, plasmids, microspheres, and live attenuated bacterial vectors. Notably, endostatin gene therapy delivered by *Salmonella* [47, 48] and *Bifidobacterium* [49] could suppress tumor angiogenesis and tumor growth in murine tumor models.

In this study, we generated an *aroA*-deficient *S. typhimurium* strain derived from a previously constructed strain, which harbors additional mutations involved in modifications of its lipid A. Upon intraperitoneal infection in mice, our constructed *aroA*-deficient strain showed greatly attenuated virulence and preferential accumulation within tumor tissue. In order to test whether newly constructed strain is suitable for delivery of antitumor agents to elicit improved therapeutic efficacy, the strain was equipped with the prokaryotic expression plasmid of one well-known anti-angiogenic agent "endostatin". The potential antitumor and adverse side effects of generated endostatin-expressing *S. typhimurium aroA*-auxotroph were evaluated in mouse models of CT26 colon carcinoma and B16F10 melanoma.

Materials and methods

Cells

The CT26 (mouse colon carcinoma) and B16F10 (mouse melanoma) cell lines were purchased from the cell bank of China Committee for Typical Culture Collection, China

Table 1 Strains and plasmids used in this study

Strains or plasmids	Descriptions	Souces
Strains		
UK-1	χ3761, the wild-type *S. typhimurium* strain	[92]
S378	Δ*rfc48*	Lab collection
S633	Δ*pagL7* Δ*pagP8* Δ*lpxR9* Δ*arnT2* Δ*eptA3* Δ*lpxT4*, derivates of χ9845	[69]
S634	Δ*pagL7* Δ*pagP8* Δ*lpxR9* Δ*arnT2* Δ*eptA3* Δ*lpxT4* Δ*aroA8*	S633
S636	Δ*pagL7* Δ*pagP8* Δ*lpxR9* Δ*arnT2* Δ*eptA3* Δ*lpxT4* Δ*aroA8* Δ*asd-66*	S634
E. coli χ7232	*endA1 hsdR17 (rK−,mK+) supE44 thi-1 recA1 gyrArelA1*D *(lacZYA-argF) U169*λpir*deoR* (*'80dlac* D *(lacZ) M15*)	[93]
E. coli χ7213	thi-1 thr-1 leuB6 glnV44 tonA21 lacY1 recA1 RP4-2-Tc::μλpir D*asdA4* D*zhf-2*::Tn 10	[93]
Plasmids		
pYA4278	*SacB* mobRP4 R6K ori Cm^+, pRE112-T-vector	[52]
pSS262	Δ*aroA* suicide plasmids	pYA4278
pSS021	Δ*asd* suicide plasmids	Lab collection
pYA3342	Asd + pBR ori Ptrc	[94]
pYA3342-ES	Endostatin-expressing plasmids	pYA3342

Academy of Sciences. Cells were grown in RPMI 1640 (CT26) or high-glucose DMEM (B16F10) supplemented with 10% FBS (fetal bovine serum) and 1% penicillin–streptomycin, and cultured at 37 °C in a humidified atmosphere of 5% CO_2. Cells were counted using a Fuchs–Rosenthal counting chamber and seeded into 24-well plates (2×10^5 cells per well), six-well plates (5×10^5 cells per well), or 75 cm^2 culture dishes (5×10^6 cells per dish). The culture medium was changed every 2 days until cells reached 80% confluence.

Bacterial strains and plasmids

The bacterial strains and plasmids used in this study are listed in Table 1. Suicide vector technology was used to generate precise deletion mutations. Two primer pairs, D*aroA*-1F/D*aroA*-1R and D*aroA*-2F/ D*aroA*-2R, were used to amplify approximately 400-bp DNA fragments upstream and downstream of the *aroA* gene. These two fragments were fused by PCR using primers D*aroA*-1F and D*aroA*-2R. The fused PCR product was cloned into pYA4278 to construct a new suicide plasmid (pSS262). The deletion of *aroA* was introduced into *S. typhimurium* strain S633 by allelic exchange using the suicide plasmid pSS262, thereby generating the *aroA*-deficient strain S634. Similarly, using the suicide plasmid pSS021, the gene "*asd*" of S634 was knocked out, generating the strain S636.

We utilized the plasmid-bacteria balanced-lethal system to ensure the stability of expression plasmids carried by *Salmonella* bacteria in vivo [50]. Briefly, we first cloned the optimized complementary DNA of human endostatin into the open reading frame of the empty plasmid pYA3342, which is with the *asd*-complementary background, thereby constructing the endostatin-expressing plasmid pYA3342-endostatin (thereafter, "pES" for short). Then, by introducing the plasmid pES into the strain S636, the endostatin-expressing *aroA*-deficient strain was generated (S636/pES).

Preparation of *Salmonella* bacteria for in vitro and in vivo experiments

All bacterial strains were cultured on LB agar plates or in LB broth containing appropriate antibiotics. A single colony of strains was picked, inoculated into LB broth, and grown overnight in a shaking incubator (37 °C, 180 r.p.m.). The next day, the overnight culture was diluted 100-fold into fresh medium to grow to exponential phase with an optical density value at 600 nm (OD_{600}) of 0.8–0.9. The bacterial cells were then collected by centrifugation (4000×*g* for 10 min), washed with phosphate buffer saline (PBS), quantified by spectrophotometry, and diluted in PBS to obtain the desired concentration of bacteria in an appropriate volume for the in vitro and in vivo experiments. The bacterial count was calculated as follows: 1.0 $OD_{600} = 0.8 \times 10^9$ CFU.

Determinations of bacterial phenotypes

The phenotypes of bacterial strains including the lipid-A-modified strain S633, the *aroA*-deficient strain S634, and the wild-type *S. typhimurium* strain UK-1 were determined in vitro and assays were repeated at least twice. The growth rates of bacterial strains in LB medium in a shaking

incubator (37 °C, 180 r.p.m.) were measured every 1 h, with an initial OD_{600} value of 0.03.

LPS profiles of *Salmonella* strains were examined by the method of Hitchcock and Brownusing cultures standardized based on the OD value at 600 nm [51].

Bacterial sensitivity to human complement was tested as described before [52]. Briefly, 50 μL of bacterial suspensions containing about 2×10^7 CFU *Salmonella* were added to 50 μL of non-treated sera or heat-inactivated sera (HIS) (1:1) and the mixture was incubated for 30 min at 37 °C. Serial dilutions of the samples in PBS were plated on LB plates and incubated overnight at 37 °C. The CFU of alive bacteria were determined. Human blood was taken from volunteers and heat-inactivated serum was prepared for 2 h at 56 °C as a control. The *rfc* mutant S378, the LPS of which contains only one O-unit, was used as the positive control to prove the bactericidal activity conferred by complement components of non-treated sera.

Swarming motility was assessed on LB plates solidified with 0.3% agar (wt/vol) as described previously [52]. In brief, 6 μL of bacterial suspension (~1×10^6 CFU) was spotted onto the middle of the semi-solid plates and subsequently incubated at 37 °C for 6 h. The diameters of the swarming colonies were measured. The plates containing 0.3% agar were allowed to dry at room temperature for 2 h and freshly grown bacteria were collected from LB agar plates followed by washing and dilution in PBS.

Invasion assays for determining bacterial infection in cancer cells were performed as described previously [53]. The CT26 and B16F10 cells were seeded into the individual wells of 24-well plates 16 h prior to infection, to obtain a density of 5×10^5 cells per well. A total of 5×10^7 of CFU of bacterial strains prepared as described above were added to cancer cells to achieve the desired multiplicity of infection (100:1), and the mixture was incubated at 37 °C under 5% CO_2 for 2 h. Following three times of washing with PBS, tumor cell line-optimal medium containing gentamycin (200 μg/mL; Sigma) was added and cells were incubated for additional 1 h to kill extracellular bacteria. Intracellular bacteria were then collected after washing and extraction with the lysis buffer (0.05% Triton X-100 diluted in PBS). The lysate was diluted in PBS and plated onto LB plates and the plates were incubation at 37 °C overnight before enumeration of the CFU of alive bacteria.

Immunofluorescence analysis

Indirect immunofluorescent assays were performed to determine the invasion of S636/pES in tumor cells and the expression of endostatin. Cells were seeded into six-well plates containing cover slips and cultured for 16–24 h before use. Bacterial strains were grown and prepared as described above. The collected bacteria were washed twice with PBS, diluted in serum-free medium, and added to cancer cells at a ratio of 100:1. After incubation of the mixture at 37 °C under 5% CO_2 for 2 h, the cells were washed with PBS, and further cultured with gentamycin-containing medium for 1 h to kill extracellular bacteria. Then, the cells were washed gently with PBS, fixed in 4% paraformaldehyde, and stained with a rabbit anti-*Salmonella* polyclonal antibody (dilution, 1:500; catalog no. ab156656, Abcam) for 12 h at 4 °C. The goat anti-rabbit immunoglobulin G polyclonal antibody conjugated with Alexa Fluor 488 (dilution, 1:100; catalog no. ab150077, Abcam) were added and the slides were incubated for 1 h at room temperature. For the staining of endostatin, mouse anti-endostatin monoclonal antibody and goat anti-mouse polyclonal antibody conjugated with Alexa Fluor 647 (dilution, 1:100; catalog no. ab150115, Abcam) were used. CytoPainter Phalloidin-iFluor 555 Reagent (dilution, 1:1000; catalog no. ab176756, Abcam) and DAPI (dilution, 1:100; catalog no. R37606, Invitrogen) was applied to indicate cell boundaries and nuclei, respectively. The cells were observed under a confocal microscope.

Western blot analysis of the expression of endostatin by S636/pES

The expression of endostatin by S636/pES was analyzed by western blotting. Bacterial pellets were boiled for 5 min in loading buffer and subjected to 12% SDS-PAGE (sodium dodecyl sulfate-polyacrylamide gel electrophoresis) and then transferred to nitrocellulose membranes (Bio-Rad, China). The membranes were probed with a mouse anti-endostatin monoclonal antibody (dilution, 1:2000; catalog no. MA1-40230, Themofisher), followed by a horseradish peroxidase (HRP)-conjugated anti-mouse secondary antibody (dilution, 1:2000; catalog no. 1030-05, Southern Biotech). Immunoreactive proteins were detected using ECL western blotting substrate (catalog no. 32209, Themofisher) and visualized by an image reader machine.

Animals

Six-to seven-week-old female BALB/c and C57BL/6 mice (20–25 g) were purchased from Dashuo Biotechnology Co., Ltd. (Chengdu, China). Animal care, experiments, and killing were performed following the principles stated in the Guide for the Care and Use of Laboratory Animals. All efforts were made to minimize animal suffering during the experiments. The mice were acclimated for 7 days after arrival before experiments started.

For the establishment of tumor models in mice, CT26 (5×10^5) and B16F10 (2×10^5) cells were collected and suspended in 100 μL of PBS respectively prior to subcutaneous injection into the right back of each mouse. The

CT26 and B16F10 cell lines were used to establish colon carcinoma models in BALB/c mice and melanoma models in C57BL/6 mice, respectively. When tumor volumes of mice reached about 200 mm^3, tumor-bearing mice were grouped randomly and received scheduled treatments.

Determination of bacterial virulence in mice

The 50% lethal doses (LD_{50}s) of *Salmonella* bacterial strains of S633, S634, and UK-1 were determined in BALB/c mice as previously described [52]. Freshly grown bacteria were collected, washed, and diluted to the required inoculum density in PBS by adjusting the OD_{600} value of bacterial suspension. Groups of five mice each were infected intraperitoneally or orally with various doses of the wild-type *S. typhimurium* strain, or its derivatives used in this study (i.e., S633 and S634) in a volume of 100 or 20 μL, ranging from 1×10^2 to 1×10^9 CFU. The mice were observed for 4 weeks post infection and deaths were recorded daily. Experiments were repeated two times. The LD_{50}s of different strains were calculated with the software SPSS.

Colonization of engineered *Salmonella*

In the colonization experiment, subcutaneous tumor models of colon carcinoma were established in BALB/c mice. When tumor volumes of mice reached about 200 mm^3, 100 μL of bacterial suspension containing 5×10^6 CFU of S633 or S634 bacteria, or PBS was injected into each mice (day 0). Tumor-bearing mice were then killed at the indicated dpi (dpi 1, 3, 7, 14, 21), and tissues of spleen, liver and tumor were taken to determinate bacterial burden. Tissue samples were homogenized and diluted in PBS, and dilutions of 10^1 to 10^7 (depending on the tissues) were plated onto LB plates containing appropriate antibiotics to determine the number of viable bacteria. The bacterial burden within normal and tumor tissues was expressed as CFU per g tissue. Colonization experiments were repeated twice.

Therapeutic benefits

The possible therapeutic benefits of S636 carrying endostatin-expressing or empty plasmids were evaluated in CT26 colon carcinoma and B16F10 melanoma-bearing mice successively. Tumor-bearing mice were randomly divided into three groups (termed "S636/pES", "S636/pEmpty", and "PBS", respectively) of eight mice each and 100 μL of bacterial suspension (5×10^6 CFU) or PBS was injected into each of mice intraperitoneally. The tumor volumes of mice of different groups were measured with a caliper every 2 days. Tumor volume (mm^3) was estimated using the formula $(L \times W^2 \times \pi)/6$, where L is the length and W is the width of the tumor in millimeters. Mice with CT26 tumors exceeding 1500 mm^3 were scheduled for euthanasia. For the mouse melanoma model, tumor volumes and survival of mice were recorded until serious illness appeared. Meanwhile, body weights of tumor-bearing mice were measured as an indicator for general health status. Animal experiments for evaluation of therapeutic antitumor benefits of our construct were performed twice and the results were taken together for analysis.

Histological and immunohistochemical studies

During animal experiments, four CT26 tumor-bearing mice of each group were killed at 14 dpi and normal and tumor tissues were taken for histological and immunohistochemical studies. Tissue samples were fixed immediately with 4% paraformaldehyde. Standard hematoxylin and eosin staining of paraffin-embedded tissues was performed for pathological examination. For the immunohistochemical staining, heat-induced antigen retrieval was performed at temperature >95 °C in 10 mM sodium citrate buffer (pH 6.0) and followed by cooling down at room temperature. Endogenous peroxidase activity was quenched by incubating the sections with 3% hydrogen peroxide for 10 min. After that, the sections were blocked with blocking buffer (0.1% Triton X-100, 3% BSA, and 2% normal donkey serum) for 1 h, and incubated with following primary antibodies: anti-*Salmonella* (Abcam), anti-endostatin (Themofisher), anti-CD34 (catalog no. ab185732, Abcam), and anti-Caspase-3 (catalog no. ab13847, Abcam). After washing with PBS, HRP-conjugated secondary antibodies were added. Then, the sections were stained with a freshly prepared 3,3′-diaminobenzidine (DAB) chromogen and counterstained with hematoxylin. Photos were taken in five random fields of each sample under a digital microscope by using a bright-field illumination. For immunohistochemical sections, the integrated optical density of positive staining was tested by the software Image-Pro Plus 6.0.

Statistical analysis

Numerical data were expressed as means ± SEM. One-way analysis of variance followed by Dunnett's or Bonferroni's multiple comparison test was used to evaluate bacterial motility, invasion activities, colonization profiles, therapeutic benefits, and clinical chemistry parameters for multiple comparisons among groups. The Kaplan–Meier method was used for survival, and differences were analyzed by the log-rank test. All analyses were performed using GraphPad Prism 5.0. $P < 0.05$ was considered as statistically significant (*, #, or †); $P < 0.01$ as very significant (**, ##, or ††); and $P < 0.001$ as extremely significant (***, ###, or †††).

Results

Construction of the *aroA*-deficient *S. typhimurium* strain and evaluation of its phenotypes

In this study, we aimed at generating an attenuated *S. typhimurium* strain with high tumor-targeting for cancer therapy. We used previously constructed strain S633 (Δ*pagL7* Δ*pagP8* Δ*lpxR9* Δ*arnT2* Δ*eptA3* Δ*lpxT4*) (Table 1), of which the LPS was characterized in homogeneous hexa-acylated lipid A. For further attenuation, we introduced the deletion of *aroA* into S633 and thereby generated the strain S634, which was auxotrophic for aromatic amino acids and unable to grow in minimal salt media (data not shown). We evaluated the virulence of bacterial strains by determining their intraperitoneal LD_{50}s in BALB/c mice, and revealed that the virulence of S633, whose LD_{50} is 5.3×10^3, was reduced by at least 20-fold compared to the wild-type strain UK-1, whose LD_{50} is $<3 \times 10^2$, and S634, whose LD_{50} is 1.2×10^7, was >2000-fold attenuated when compared to its parent strain S633. The oral LD_{50}s of S633 and S634 were both larger than 10^9, indicating these two mutants are avirulent compared to the wild-type strain UK-1 (Table 2).

Bacterial growth curves were evaluated in LB broth, and it was shown that S634 grew more slowly than its parent strain S633 and the wild-type strain UK-1 (Supplementary Fig. S1). All cultures grew to stationary phase after 8 h of shaking culture (37 °C, 180 r.p.m.), despite of slight differences among the OD values of different cultures in the platform period. The deletion of *aroA* did not seem to affect the LPS phenotype (Fig. 1a) or the sensitivity to serum complement (Fig. 1b). S634 showed decreased motility on semi-solid agar plates by about one-third compared to its parent strain, as determined by the diameter of swarming motility (Fig. 1c). To test the interaction between *Salmonella* bacteria and the tumor, cancer cells of the CT26 and B16F10 cell lines were incubated with S633, S634, and UK-1 in vitro. It was shown that the ability of the *aroA*-deficient strain S634 to invade the CT26 and B16F10 cells was decreased, compared to S633 and UK-1 (Fig. 1d). In addition, the declined growth rate and the decreased ability to invade cancer cells were at least partly recovered by introduction of *aroA*-complementary plasmids into the *aroA*-deficient strain (data not shown).

Table 2 LD_{50}s of *S. typhimurium* on mice

Strains	Intraperitoneal LD_{50}	Oral LD_{50}
S633	5.3×10^3	$>10^9$
S634	1.2×10^7	$>10^9$
UK-1	$<3 \times 10^2$	5×10^4

Engineered *S. typhimurium* specifically colonizes tumor tissue in vivo

Colonization experiments were conducted to determine the tumor-targeting ability of the *aroA*-auxotrophic strain S634 in subcutaneous tumor models of colon carcinoma. On the 1st, 3rd, 7th, 14th, and 21st day after tumor-bearing mice received intraperitoneal infection of bacterial strains, the samples of tumor, liver, and spleen were taken and bacterial burdens were determined. At dpi 1, between 1×10^4 and 1×10^6 CFU/g of S634 were observed in normal tissues (liver and spleen) and about 1×10^8 CFU/g in tumor tissue. After that, bacterial burdens in the liver and spleen tissues were decreased gradually (Fig. 2a, b), but remained relatively stable in tumor tissue (Fig. 2c). The strain S634 preferentially accumulated in tumor tissue compared to normal tissues, with tumor-to-normal tissue (liver) ratios ranging from 1500:1 to over 100,000:1 throughout the experiment (Fig. 2d). However, the parent strain S633 colonized tumor tissue with low specificity (tumor-to-liver ratio ≈ 10:1) before the mice succumbed to its infection (data not shown).

S636/pES can express endostatin and invade cancer cells in vitro

In this study, we attempted to test whether the strain S634 is suitable to deliver therapeutic antitumor agent "endostatin", one of the most potent inhibitors of angiogenesis. We constructed the endostatin-expressing plasmid named "pES" (asd^+) and introduced it into S636, the asd^- derivative of tumor-targeting S634, thereby generating S636/pES, in which plasmids and bacterial strains form a balanced-lethal system. The expression of endostatin in *Salmonella* bacteria S636 was confirmed in vitro by western blotting (Fig. 3a). The immunofluorescence assay also demonstrated that S636/pES could invade both CT26 and B16F10 tumor cells (Fig. 3b) and express endostatin (Fig. 3c). Notably, to avoid the loss of expression plasmids carried by *Salmonella* bacteria in vivo, we utilized the plasmid-bacteria balanced-lethal system in this study [50], showing that the plasmid stability was nearly 99% in vitro and in vivo (data not shown).

Combination of *S. typhimurium* and endostatin inhibits tumor growth and improves the survival of tumor-bearing mice

Animal experiments were performed in CT26 colon carcinoma- and B16F10 melanoma-bearing mice to study the potential therapeutic benefits elicited by the our *Salmonella* mutant and endostatin. When tumor sizes reached about 200 mm^3, tumor-bearing mice were grouped randomly and

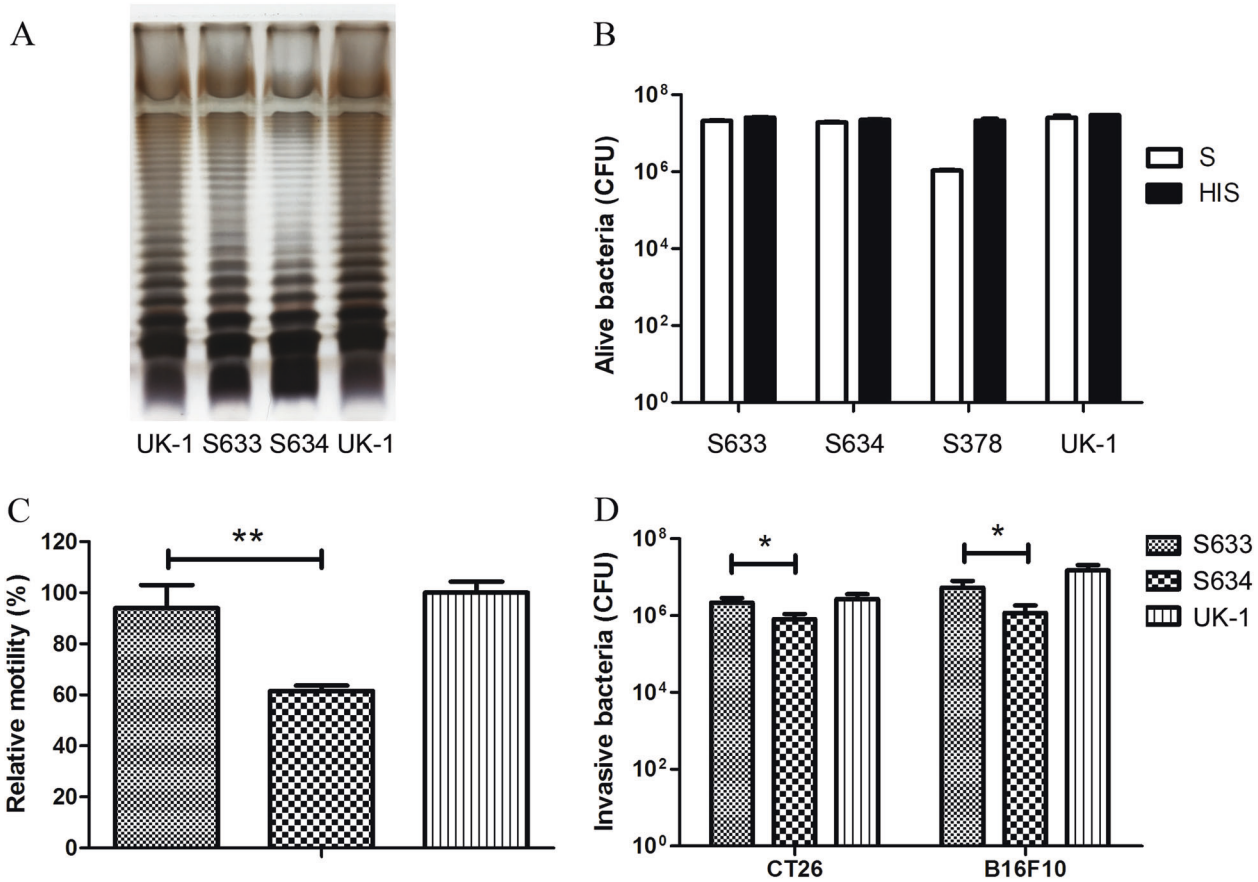

Fig. 1 Phenotypic characterization of engineered *S. typhimurium*. **a** LPS phenotypes of bacterial strains were identified by silver staining. **b** In vitro sensitivity toward human complement. Bacteria (2×10^7 CFU) were treated with either untreated or heat-inactivated (HI) human serum for 30 min at 37 °C. **c** Swarming motility of bacterial strains was assessed on 0.3% semi-solid agar. Relative motility of S633 and S634 was calculated by comparing with the wild-type strain UK-1. **d** Invasion of bacterial strains in cancer cells. Values represented the number of *Salmonella* bacteria that invaded cancer cells and significant differences were determined. The significance of differences among different groups were analyzed by the one-way ANOVA test and Bonferroni's multiple comparison test and indicated by asterisks (*$P < 0.05$; and **$P < 0.01$)

received 5×10^6 CFU of S636/pES, S636/pEmpty, or 100 µL of PBS intraperitoneally. In CT26 tumor models, S636/pES showed stronger suppressive effects on tumor growth compared with S636/pEmpty at dpi 12 ($P < 0.05$, S636/pES versus S636/pEmpty) and 14 ($P < 0.01$) (Fig. 4a). At 12 dpi, the mean tumor volume of the PBS group was about 1600 mm^3, whereas those of the S636/pEmpty and S636/pES groups were 1100 mm^3 ($P < 0.01$, versus the PBS group) and 600 mm^3 ($P < 0.001$, versus the PBS group), respectively (Fig. 4a). Then, we established aggressive B16F10 melanoma models for further validation. Similarly, mice of the S636/pES group showed significantly superior therapeutic benefits compared to mice treated with S636/pEmpty at dpi 12, 14, 16, and 18 ($P < 0.05$, or $P < 0.01$, S636/pES versus S636/pEmpty) (Fig. 4b). After 2 weeks (at dpi 14), the mean tumor volume of the PBS group was about 2800 mm^3, whereas those of the S636/pEmpty and S636/pES groups were about 1750 mm^3 ($P < 0.01$, versus the PBS group) and 850 mm^3 ($P < 0.001$, versus the PBS group), respectively (Fig. 4b). Moreover, the survival of B16F10 tumor-bearing mice was obviously prolonged by treatments with S636/pES and S636/pEmpty ($P < 0.01$ and $P < 0.001$, respectively, versus the PBS group) as shown in Fig. 4c. Mice treated with S636/pES survived for the longest period of time, which is nearly 31 days, followed by S636/pEmpty-treated mice for 24 days ($P < 0.05$, S636/pES versus S636/pEmpty), whereas PBS-treated tumor-bearing mice were alive only for 15 days on the average (Fig. 4c). Taken together, engineered *S.* typhimurium carrying endostatin expression plasmids (i.e., S636/pES) exerted significant antitumor effects on both mouse tumor models. Furthermore, S636 carrying empty plasmids (S636/pEmpty) could also obviously suppress tumor growth and prolong the survival of melanoma-bearing mice, though its antitumor efficacy was not quite as powerful as that of S636/pES.

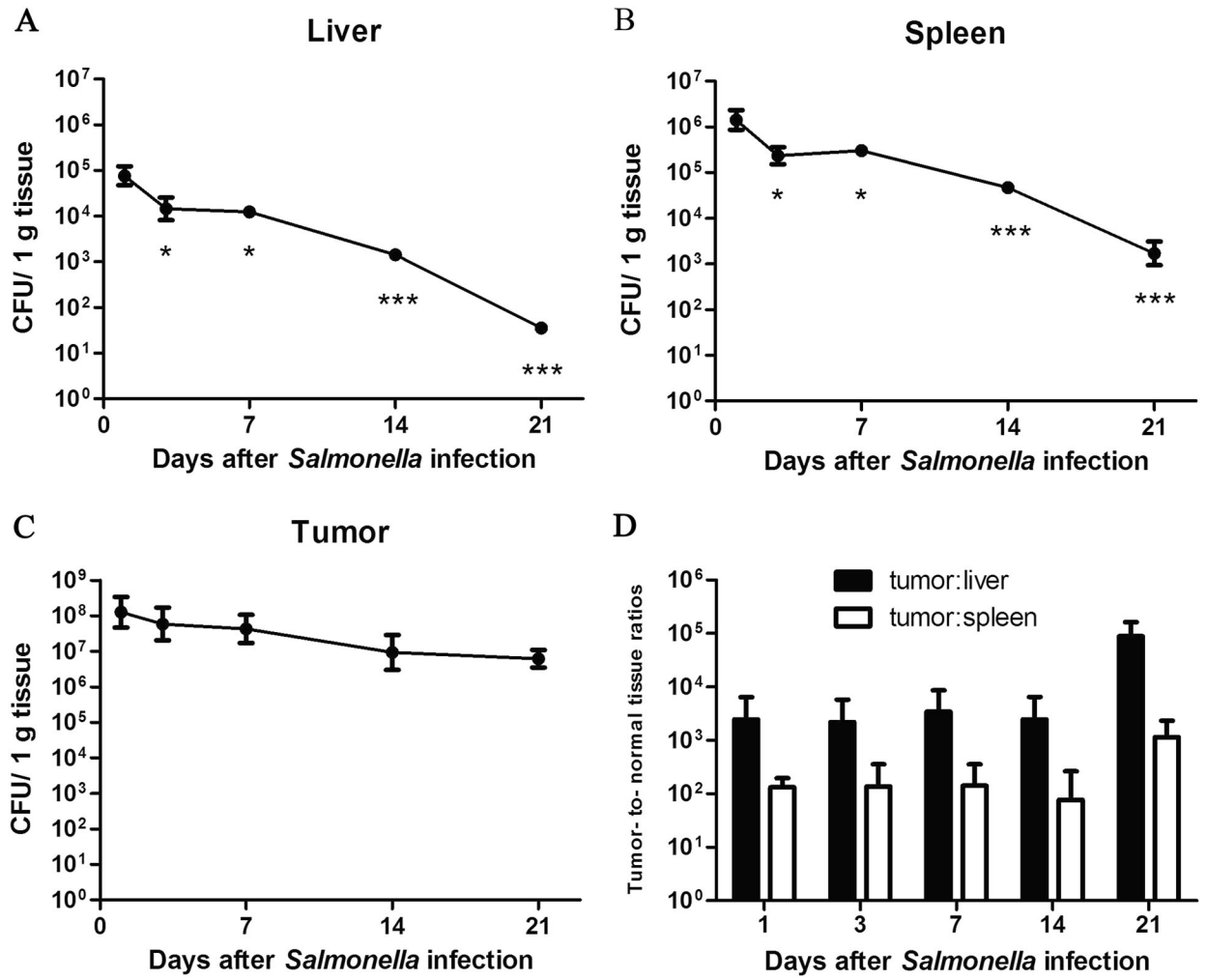

Fig. 2 The colonization profile of S634 in tumor and normal tissues. For determination of the tumor-targeting ability of S634, four tumor-bearing mice were killed at each indicated dpi, and tumor and normal tissues were taken sterily. Bacterial burdens in the liver (**a**), spleen (**b**) and tumor tissues (**c**) were determined by plating serial dilutions of tissue homogenates and expressed as CFU g-1 tissue. **d** Tumor-to-normal tissue ratios were shown at different dpi. Bacterial burdens at different dpi shown in **a**–**c** each are compared with the values at dpi 1 by the one-way ANOVA test and Dunnett's post-test (*$P < 0.05$; **$P < 0.01$; and ***$P < 0.001$)

S636/pES inhibits angiogenesis and increases apoptosis within tumor tissues

Tumor samples were taken for immunohistochemical studies 2 weeks after tumor-bearing mice received treatments. Corresponding to the colonization experiments, S636 carrying either empty or endostatin-expressing plasmids could colonize the tumor after systemic infection, which was indicated by immunohistochemical staining for *Salmonella* (Fig. 5a, b). Besides, the expression of endostatin within tumor tissues was detected when mice were treated with S636/pES (Fig. 5a, b).

Since suppression of tumor growth is always accompanied by activation of apoptosis within tumor tissue, we analyzed the apoptosis by immunohistochemical staining for a cleaved form of caspase-3 (Fig. 5a), which is a key enzyme activated in the apoptosis pathway [54]. Compared with the PBS group, the S636/pES and S636/pEmpty groups showed significantly elevated apoptosis in tumor tissues, which was indicated by the increased level of activated caspase-3 (Fig. 5c). To determine if the expression of endostatin within tumor tissue elicited anti-angiogenic effects, we performed the staining for CD34, which is mainly expressed on small vessel endothelial cells and tumors of epithelial origin [55]. The expression level of CD34 that indicated the microvessel density was significantly decreased within tumor tissues of the S636/pES group compared to the PBS and S636/pEmpty groups (Fig. 5c). Thus, it was plausible that the accumulation of *Salmonella* bacteria and the expression of endostatin within tumor tissue elicited effects of apoptosis induction and anti-angiogenesis respectively, which at least partly explained the superior therapeutic benefits elicited by S636/pES than S636/pEmpty.

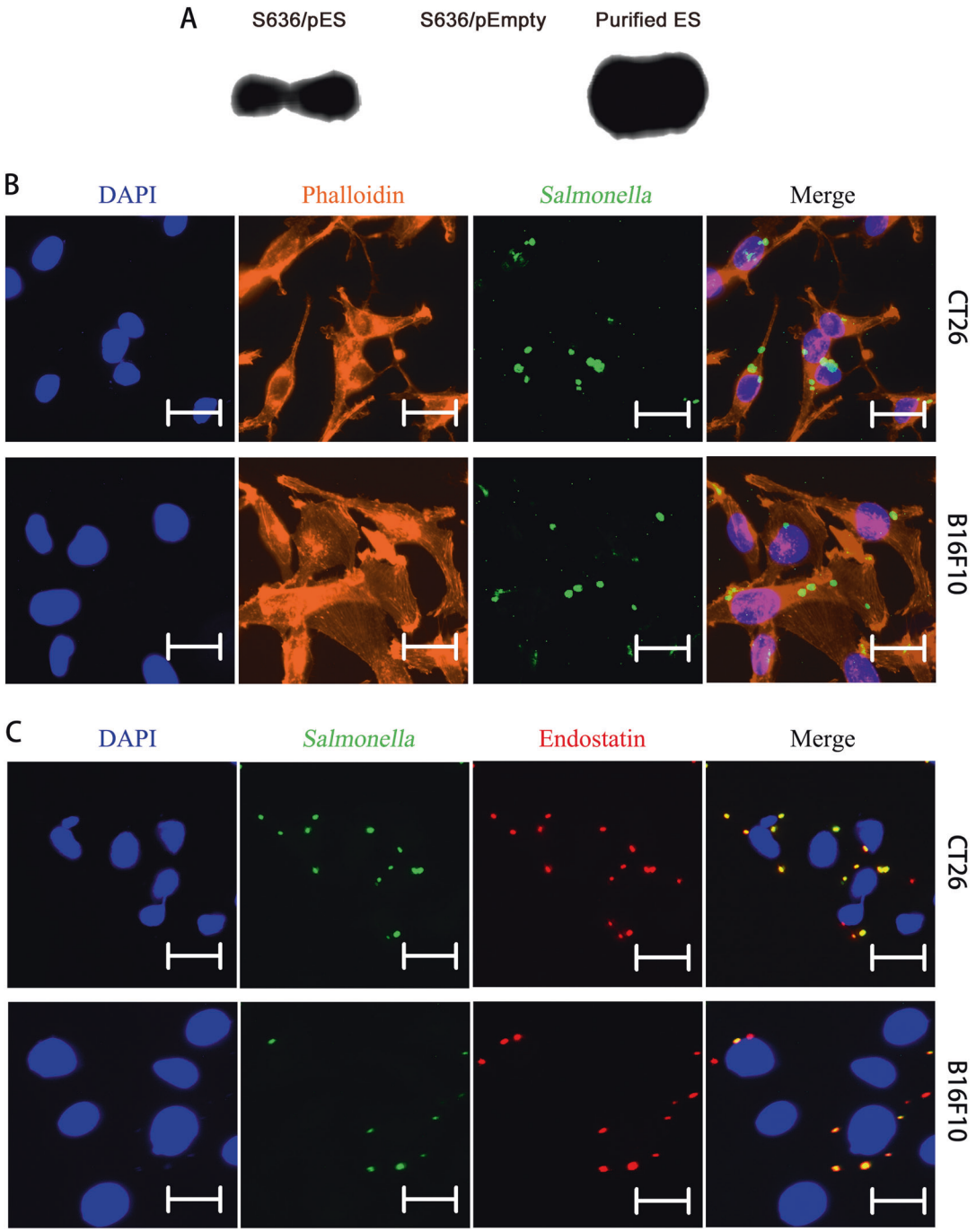

Fig. 3 Endostatin expression and invasion of S636/pES in cancer cells. **a** The expression of endostatin was analyzed by western blotting. The invasion of S636/pES in tumor cells (**b**) and the expression of endostatin (**c**) were determined by immunofluorescence assays. Tumor cells were infected with S636/pES for 2 h with an MOI of 100:1, and further cultured with gentamycin-containing medium for 1 h to kill extracellular bacteria. For visualization by confocal microscopy, cell nuclei (blue) and actin (orange) were stained with DAPI and Phalloidin, respectively. *Salmonella* (green) and endostatin (red) were stained by corresponding antibodies as well. Scale bar, 20 μm

Adverse side effects of engineered *S. typhimurium*

During animal experiments, we also monitored the general health of tumor-bearing mice, as indicated by the body-weight change of mice. The body weights of mice were decreased by about 10% within the initial 2 days after treatment with S636/pES and S636/pEmpty while gradually recovered later, which took about 1 week (Fig. 6). It seems plausible to speculate that intraperitoneal infection of the *aroA*-deficient *Salmonella* bacteria S636 did elicit severe toxicity to the mice, while the administration dose adopted (5×10^6 CFU) in this study was tolerable for those tumor-

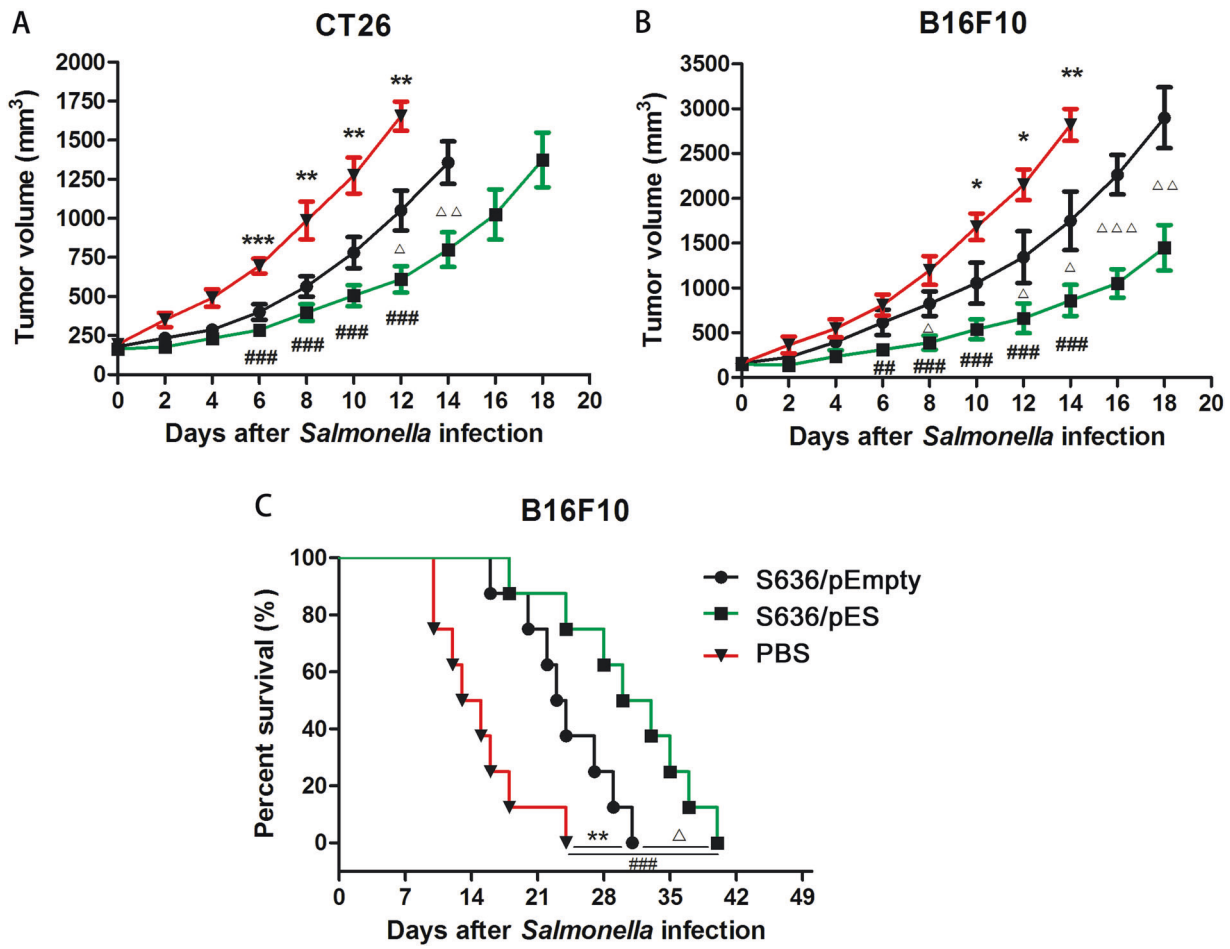

Fig. 4 Tumor-suppressive effects of S636 with empty or endostatin expression plasmids. When tumors reached ~200 mm^3, mice were randomly divided into three groups of eight mice each and intraperitoneally injected with PBS, S636/pEmpty, or S636/pES. Tumor volumes of CT26 colon carcinoma-(**a**) and B16F10 melanoma-(**b**) bearing mice were measured every 2 days. The error bars represent the mean ± SEM. **c** Kaplan–Meier survival curves for mice bearing B16F10 melanoma were monitored and differences among three groups were analyzed by the log-rank test. One-way ANOVA analysis followed by Bonferroni's multiple comparison test was used to evaluate and compare therapeutic antitumor benefits elicited by S636/pEmpty or S636/pES on tumor-bearing mice. The significance of differences among all groups in the mean tumor volumes or survival time were analyzed, and the asterisk (*), hash symbol (#), and triangle (†) represented S636/pEmpty versus PBS, S636/pES versus PBS, and S636/pEmpty versus S636/pES, respectively. *, #, or †, $P < 0.05$; **, ##, or ††, $P < 0.01$; and ***, ###, or †††, $P < 0.001$

bearing mice. Meanwhile, we also took samples of blood and normal tissues including liver and spleen from tumor-bearing mice at 14 dpi for studies. Pathologic examination by hematoxylin and eosin staining showed that, treatment with S636/pES and S636/pEmpty caused pathological changes to some extent on normal tissues, which indicated by the swelling and degeneration of hepatocytes in the liver and the inflammation in the spleen (Fig. 7).

Discussion

Bacteria-mediated tumor therapies aim at overcoming some of the shortages or limitations of conventional treatments, such as low tumor-targeting and damage to normal tissues or cells. *S. typhimurium*, as facultative anaerobic bacteria, are good candidates of therapeutic antitumor agents and have been commonly used in bacteria-mediated tumor therapy. As *S. typhimurium* with intrinsically pathogenic properties may cause serious toxicity to the body especially after systemic infection, it is necessary to attenuate such bacteria adequately before clinical studies. One of the strategies for bacterial attenuation is via auxotrophic mutations. *aroA* gene is responsible for the synthesis of aromatic amino acids, which are not freely available in the mammalian host. Thus, deletion of *aroA* results in *Salmonella* bacteria auxotrophic, leading to increased immunogenicity and adjuvant potential, and has been commonly used to attenuate such bacteria [23]. In this study, we constructed a fine-defined *aroA*-deficient *S. typhimurium* strain, accompanied with additional mutations including Δ*pagL7* Δ*pagP8* Δ*lpxR9* Δ*arnT2* Δ*eptA3* Δ*lpxT4*, which

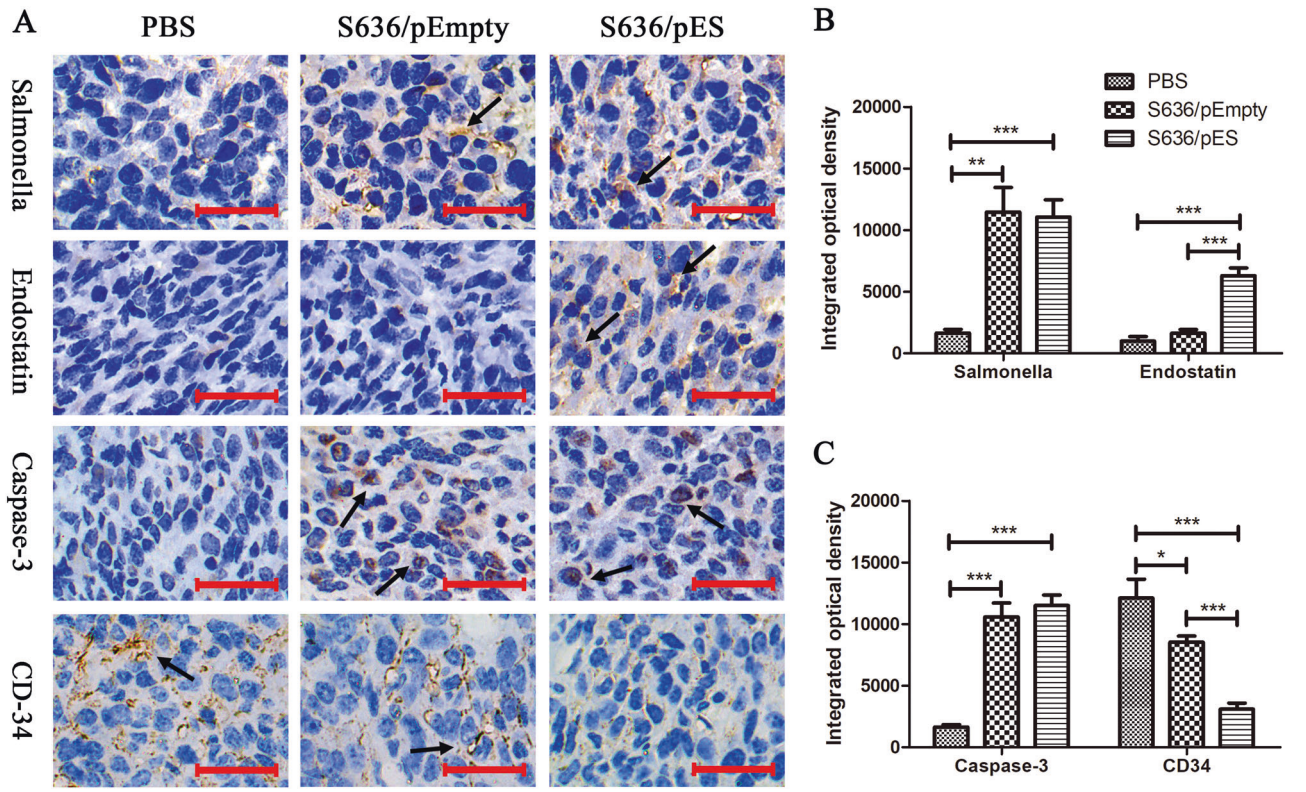

Fig. 5 Immunohistochemical (IHC) studies on tumor tissues. Two weeks after tumor-bearing mice received treatment of S636/pES, S636/pEmpty, or PBS intraperitoneally, tumor samples were taken for immunohistochemical studies as described above. **a** The accumulation of *Salmonella* bacteria and the expression of endostatin within tumor tissues were determined by immunohistochemical staining for *Salmonella* and endostatin, respectively. Tumor microvascular density (MVD) and the apoptosis levels within tumor tissues of different groups were tested by stainings of CD34 and activated caspase-3, respectively. Positive staining was indicated by the black arrow. Scale bar, 40 μm. The positive staining for *Salmonella*, endostatin (**b**), caspase-3, and CD34 (**c**), each was semiquantitatively analyzed by the software Image-Pro Plus 6.0 and indicated by the integrated optical density (IOD) value. The significance of differences among different groups were analyzed by the one-way ANOVA test and Bonferroni's multiple comparison test and indicated by asterisks ($*P < 0.05$; $**P < 0.01$; and $***P < 0.001$)

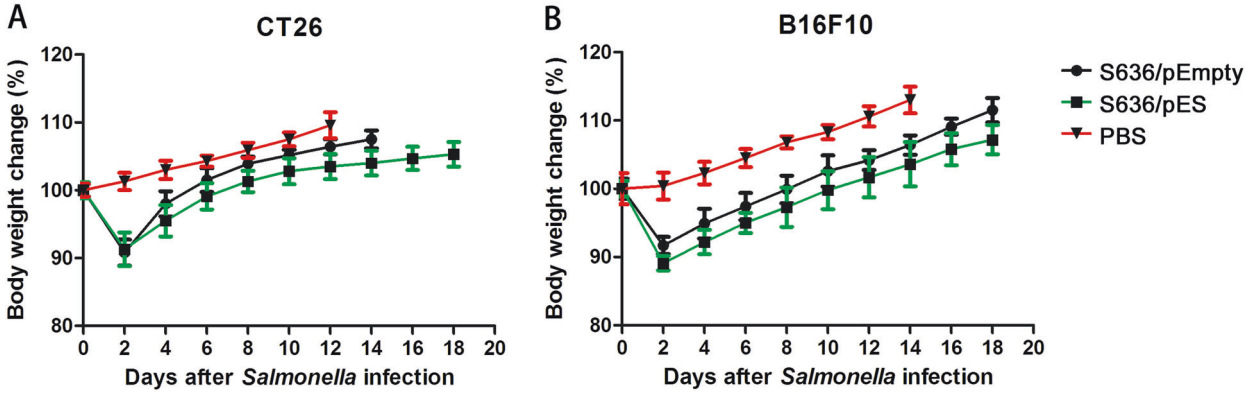

Fig. 6 The body-weight changes of tumor-bearing mice. During animal experiments, body weights of CT26 (**a**) and B16F10 (**b**) tumor-bearing mice were measured as an indicator for general health status upon treatments with engineered *S. typhimurium* with empty or endostatin expression plasmids. Values at different dpi were shown as the percentages relative to the initial body weights of mice

involved in modifications of lipid A moiety of bacterial LPS. Deletion of *arnT*, *eptA*, and *lpxT* genes will remove the ability of *S. typhimurium* to catalyze the addition of specific moieties (L-Ara4N, pEtN, and the second phosphate group at the 1-position), resulting in maximum exposure of two phosphate groups in lipid A to

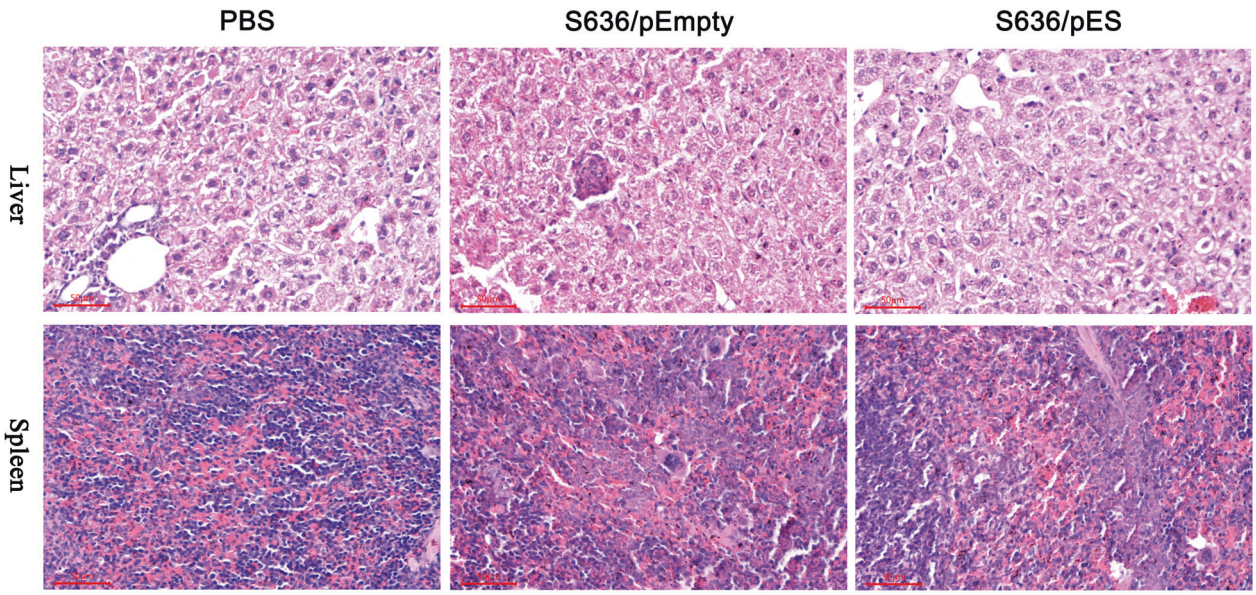

Fig. 7 Adverse side effects of engineered *S. typhimurium* on normal tissues. Pathological studies on the liver and spleen tissues were performed by standard H.E. staining. In the S636/pEmpty and S636/pES groups, the liver tissues showed disorderly arrangement of hepatic cords, which was accompanied by the swelling and degeneration of hepatocytes, and the spleen tissues appeared slight inflammation and the infiltration of phagocytic cells and inflammatory cells. There was no significant pathological change in the PBS group

facilitate its interaction with TLR4 receptor and caspase-11 [refs. 56–58]. Moreover, deletion of *pagL*, *pagP*, and *lpxR* genes enable *Salmonella* to produce hexa-acylated lipid A regardless of growing in media in vitro or in the host organ in vivo, where adverse environment such as low pH, or Mg^{2+}, will activate these genes to alter the number and the symmetry of acylated chains in lipid A [59, 60]. These six gene deletions will ensure the lipid A integrity and maintain its most potent stimulatory structure in live *Salmonella* bacteria during its invasion, colonization, and persistence in the host gut-associated lymphoid tissues and in tumor tissues.

Thus, a new live *Salmonella* strain was constructed for cancer therapy and as a vector to deliver antitumor agents. As expected, the virulence of the *aroA*-deficient strain S634 in mice was significantly reduced, as shown by the LD_{50} value of 1.2×10^7, over 2000-fold increase of LD_{50} compared with that of the strain S633 upon intraperitoneal infection, and S634 was avirulent by oral route due to mutations of *aroA* and *arnT* and *eptA* (Table 2). Besides the significant reduced virulence, a good *Salmonella* candidate for tumor therapy should possess other properties such as ability to migrate toward the tumor, penetrate into tumor tissue, and colonize the tumor in large amounts. An in vitro model of continuously perfused tumor tissues indicated that motility and bacterial chemotoxis mediated by chemoreceptors were critical for directing *Salmonella* to migrate toward the different microenvironment regions of tumor cells, and *Salmonella* with higher motility have enhanced penetration and colonization within tumor tissues [61, 62]. In our study, we revealed that the motility of S634 was decreased by about one-third compared to that of its parent strain (Fig. 1c), consistent with the recent observation [23]. But this motility deficiency in our construct did not compromise its ability to accumulate within tumor tissue in mouse model because S634 still showed the good ability to invade tumor cells in vitro, and S634 also preferentially colonized tumor tissue relative to normal tissues in vivo with tumor-to-liver ratios ranging from 1500:1 to over 100,000:1 (Figs. 2d and 3), indicating that the motility may not play an essential role in mediating its migration toward tumor tissues. Recent studies using mouse tumor models showed that bacterial colonization and migration process within the tumor in mice was a passive mechanism dramatically influenced by inflammatory cytokines and bacterial metabolism of *Salmonella* [63–65]. This could explain that most of *Salmonella* mutants in random mutants screen showing the great ability to preferentially proliferate throughout tumor tissues were tied to the auxotrophic mutations mostly associated with requirement of aromatic amino acid, leucine and arginine synthesis [21, 66]. However, whether the motility mediated by flagellum is vital for directing *Salmonella* to migrate toward necrotic hypoxic/anoxic environment of tumor cells in animal model is still controversial, but it is convinced that over-expression of secreted heterologous flagellin would greatly benefit the therapeutic antitumor efficacy conferred by *Salmonella*, as demonstrated by recent work, in which, tumor-targeting *Salmonella* engineered to overexpress *Vibrio vulnificus* FlaB effectively suppressed tumor growth and metastasis

and prolonged survival in murine colon and melanoma models and these therapeutic effects were mediated by TLR4 signaling and augmented this tumor-suppressive host reactions by TLR5 signaling [67, 68].

Tumor-targeted *Salmonella* is often administered by intravenous or intraperitoneal route to induce systemic infection in tumor models, and reaching up to ratios of more than 1000:1 in cancerous tissue compared to healthy tissues (Fig. 2). Many genes, which are critical for establishing an oral infection, such as *phoP*, *invG sseD*, and *ssrB*, are not essential for intravenous infection to target, invade, and colonize the tumor cells [63], and in our study, deletion mutations of *arnT* and *eptA* genes were also proved to be required for oral infection, but not for intraperitoneal administration [69] (Table 2). However, an entire cell envelope, especially LPS, is important for *Salmonella* combatting against bactericidal activity of human complement and neutrophil clearing before attenuated *Salmonella* migrate toward and colonize tumor tissues [70, 71], because deeply rough *Salmonella* mutants showed low virulence but exhibited weak intrinsic antitumor effects [52, 72]. Our results indicated that the strain S634 exhibited the similar complete LPS pattern as the wild-type *S. typhimurium* UK-1 (Fig. 1a), explaining the similar sensitivity of the mutants to human complement (Fig. 1b) and successful invasion of S634 within tumor cells (Figs. 1d and 3).

While S634 preferentially accumulated within tumor tissue to a significant high number, this mutant still persisted in healthy tissues including the spleen and liver with comparable number for over observed 21 days (Fig. 2), indicating that only one *aroA* mutation is not sufficient for restricting *Salmonella* to replicate in the healthy tissues, other mutations are required to further decrease bacterial survival in healthy tissues for the clinical safety. The mutations associated with leucine and arginine biosynthesis are of particularly interest because these *Salmonella* auxotrophs were selected from random mutants by the ability to grow in successive tumor xenografts, and were demonstrated to receive sufficient amounts of these amino acids from the tumor environment but lose the ability to persist in the normal tissue environment [21, 66, 73]. The mutations such as *htrA*, SPI-2, and *STM3120*, are also potential candidates to reduce fitness in normal tissues and retain their fitness in tumors [74]. The novel strategy to achieve rapid elimination of bacteria from normal tissues while retaining adequate antitumor ability was developed by placing an essential gene under a hypoxia conditioned promoter [75], which can be considered for reducing bacterial load in normal tissues and increasing tumor-targeting specificity in the future work. Another interesting approach to reduce colonization in healthy organs while retaining advantages of systemic application is by an intra-tumoral route of infection, allowing the extensive dose of bacteria to bypass the killing by innate immunity encountered by systemic infection and directly target the tumor cells [76, 77].

Systemic administration of attenuated *S. typhimurium* deprives cancer cells of nutrients by competition and activates antitumor immunity, resulting in tumor regression, tumor shrinkage, and even complete tumor eradication [78, 79]. In this study, we observed therapeutic efficacy against CT26 and B16F10 tumors after intraperitoneal administration of S636/Empty and S636/pES in mouse models (Fig. 4), including inhibition of tumor growth and prolonged mouse survival, which was consistent with other studies on the antitumor effects of *S. typhimurium* and endostatin [13, 48]. But this efficacy was also accompanied by severe adverse side effects including body-weight loss and enlarged spleen of the mice, and pro-inflammatory immune responses, although the mice were recovered to normal condition later (Figs. 6 and 7). Abundant *Salmonella* persistence in the healthy organs for long time and the presence of the most potent stimulatory inflammatory lipid A in this *Salmonella* mutant are two major reasons to result in the severe side effects. Initial inflammatory response including production of tumor necrosis factor-α (TNF-α), interleukin (IL)-1β, and other cytokines induced upon systemic administration of the bacteria is a prerequisite for bacterial targeting and entrapment in tumors [7, 63, 64], subsequent accumulation and proliferation of *Salmonella* within tumors will elicit infiltration of immune cells, such as neutrophils and macrophages, to the local site of tumors tissues, and secrete pro-inflammatory cytokines such as TNF-α and IL-1β, enabling immune privileged tumor environments shift from immune suppressive to enhanced immunogenic [77, 80–82]. The inflammatory responses in these two steps appeared to be mainly mediated through TLR4 signaling activated by the lipid A of *Salmonella*, the evidences to support this notion are from the facts that macrophage and neutrophil infiltration of bacteria-colonized tumors in TLR4$^{-/-}$ mice was lower than in the wild-type mice, and administering lipid A concurrently with *Salmonella* significantly increased bacterial accumulation in both necrotic and viable tumor tissues and enhanced the antitumor capability [67, 83], and this could also partially explain the ineffectiveness of *Salmonella* VNP20009 in phase I clinical trials involving human cancer patients because of *msbB* deletion resulting in penta-acylated lipid A in *Salmonella*, an antagonist for human TLR4 while it was demonstrated its excellent antitumor capability in tumor-bearing mice model [6, 17, 84, 85]. Our results indicated that the most potent TLR4 stimulator of a hexa-acylated lipid A achieved by a deletion combination of Δ*pagL7* Δ*pagP8* Δ*lpxR9* Δ*arnT2* Δ*eptA3* Δ*lpxT4* in our constructed strains S633, S634, and S636, may not be an optimal structure used for bacteria-mediated cancer therapy because of its highest endotoxic activity, shown in Fig. 7. Considering that activation of TLR4 on the tumor cells by bacterial infection

results in tumor proliferation and progression [86], the lipid A structure with decreased activity to stimulate TLR4 signaling, such as monophosphoryl lipid A, which has been used in human clinic as vaccine adjuvants to enhance vaccine efficacy, should be investigated in the future construct as bacteria-mediated cancer therapy [69, 87–89].

Besides attenuated *Salmonella* itself as a therapeutic antitumor agent, it can express and release cytotoxic proteins, immunoregulatory proteins, and apoptosis-inducing factors, and some essential enzymes for the conversion of nontoxic prodrugs into cytotoxic drugs [78, 90]. In this study, we also tested the ability of S636, the *asd*− derivative of S634 to deliver the therapeutic antitumor protein. It has been widely recognized that angiogenesis, the formation of new capillaries from pre-existing vasculature, is one key process for tumor growth and metastasis. Thus, inhibition of angiogenesis inside tumor tissue is another promising strategy for cancer treatments. Endostatin, a 20-kDa C-terminal fragment of type XVIII collagen, is one of the most potent inhibitors of angiogenesis. Endostatin has been shown to block the proliferation and migration of endothelial cells [36] and induce endothelial cell apoptosis [37], thereby producing the anti-angiogenic activity. To employ anti-angiogenic therapy by utilizing the bacterial vector of tumor-targeting *Salmonella*, we introduced prokaryotic expression plasmids of endostatin (pES) into S636 and thereby generated endostatin-expressing *Salmonella* strain named S636/pES. The potential antitumor effects of S636/pES were evaluated in mouse CT26 colon carcinoma and B16F10 melanoma subcutaneous tumor models successively. As shown in Fig. 4a, S636/pES was able to retard the growth of CT26 tumors. Moreover, upon infection with S636/pES, the growth of aggressive B16F10 melanoma was also significantly delayed (Fig. 4b) and the survival of melanoma-bearing mice was significantly prolonged (Fig. 4c).

Previous studies have showed that endostatin can induce endothelial cell apoptosis through binding to a variety of receptors on the surface of endothelial cells. As shown in immunohistochemical studies for endostatin and CD34, when tumor-bearing mice were treated with S636/pES, the expression of endostatin within tumor tissue was accompanied by the decreased level of CD34 (compared to the S636/pEmpty and PBS groups), indicating suppression of angiogenesis (Fig. 5). Moreover, the expression level of CD34 in tumor tissues of the S636/pEmpty group was also significantly declined compared to the PBS group (Fig. 5c). It has been previously shown that after colonization, *Salmonella* would destroy local tumor blood vessels [91]. Thus, the anti-angiogenic effect of endostatin delivered by S636 probably accounted for the superior therapeutic benefits of S636/pES in tumor-bearing mice compared to S636 carrying empty plasmids.

In summary, in this study, an attenuated *S. typhimurium* mutant carrying metabolic deficiency and hexa-acylated lipid A was constructed without any genetic scars in the *Salmonella* chromosome in a modular manner, and in vivo tests demonstrated the antitumor efficacy conferred by live *Salmonella* itself and its ability to deliver the anti-angiogenic agent endostatin. Next, we will optimize this construct to maximize its capability to colonize and accumulate within tumor tissues while decreasing its adverse side effects caused by amounts of *Salmonella* bacteria in healthy tissues and endotoxic activity, and we will also optimize the delivery plasmid, enable it to express the targeted proteins under the controllable condition to maximize its therapeutic functions while reducing its toxic side effects to healthy cells.

Acknowledgements This work was funded by National Natural Science Foundation of China (grant numbers 31570928 and 31472179).

Author contributions Q.K., K.L., and Q.L. initiated the research. K.L. and Q.L. led in vitro and in vivo experimental design, data acquisition and analysis, and manuscript preparation together. P.L., Y.H., X.B., and Y.T. aided in data acquisition. Q.K. participated in experimental design, data analysis, and manuscript preparation.

Compliance with ethical standards

Conflict of interest The authors declare that they have no conflict of interest.

References

1. Chang WW, Lee CH. *Salmonella* as an innovative therapeutic antitumor agent. Int J Mol Sci. 2014;15:14546–54.
2. Malmgren RA, Flanigan CC. Localization of the vegetative form of *Clostridium tetani* in mouse tumors following intravenous spore administration. Cancer Res. 1955;15:473–8.
3. Kohwi Y, Imai K, Tamura Z, Hashimoto Y. Antitumor effect of *Bifidobacterium infantis* in mice. Gan. 1978;69:613–8.
4. Stritzker J, Weibel S, Hill PJ, Oelschlaeger TA, Goebel W, Szalay AA. Tumor-specific colonization, tissue distribution, and gene induction by probiotic *Escherichia coli* Nissle 1917 in live mice. Int J Med Microbiol. 2007;297:151–62.
5. Pawelek JM, Low KB, Bermudes D. Tumor-targeted *Salmonella* as a novel anticancer vector. Cancer Res. 1997;57:4537–44.
6. Low KB, Ittensohn M, Le T, Platt J, Sodi S, Amoss M, et al. Lipid A mutant *Salmonella* with suppressed virulence and TNF alpha induction retain tumor-targeting in vivo. Nat Biotechnol. 1999;17:37–41.
7. Forbes NS, Munn LL, Fukumura D, Jain RK. Sparse initial entrapment of systemically injected *Salmonella* typhimurium leads to heterogeneous accumulation within tumors. Cancer Res. 2003;63:5188–93.
8. Ganai S, Arenas RB, Sauer JP, Bentley B, Forbes NS. In tumors *Salmonella* migrate away from vasculature toward the transition zone and induce apoptosis. Cancer Gene Ther. 2011;18:457–66.
9. Zhang M, Forbes NS. Trg-deficient *Salmonella* colonize quiescent tumor regions by exclusively penetrating or proliferating. J Control Release. 2015;199:180–9.
10. Forbes NS. Engineering the perfect (bacterial) cancer therapy. Nat Rev Cancer. 2010;10:785–94.

11. Avogadri F, Martinoli C, Petrovska L, Chiodoni C, Transidico P, Bronte V, et al. Cancer immunotherapy based on killing of *Salmonella*-infected tumor cells. Cancer Res. 2005;65:3920–7.
12. Kaimala S, Mohamed YA, Nader N, Issac J, Elkord E, Chouaib S, et al. *Salmonella*-mediated tumor regression involves targeting of tumor myeloid suppressor cells causing a shift to M1-like phenotype and reduction in suppressive capacity. Cancer Immunol Immunother. 2014;63:587–99.
13. Jia LJ, Xu HM, Ma DY, Hu QG, Huang XF, Jiang WH, et al. Enhanced therapeutic effect by combination of tumor-targeting *Salmonella* and endostatin in murine melanoma model. Cancer Biol Ther. 2005;4:840–5.
14. Jiang T, Zhou C, Gu J, Liu Y, Zhao L, Li W, et al. Enhanced therapeutic effect of cisplatin on the prostate cancer in tumor-bearing mice by transfecting the attenuated *Salmonella* carrying a plasmid co-expressing p53 gene and mdm2 siRNA. Cancer Lett. 2013;337:133–42.
15. Fritz SE, Henson MS, Greengard E, Winter AL, Stuebner KM, Yoon U, et al. A phase I clinical study to evaluate safety of orally administered, genetically engineered *Salmonella enterica* serovar *typhimurium* for canine osteosarcoma. Vet Med Sci. 2016;2:179–90.
16. Nemunaitis J, Cunningham C, Senzer N, Kuhn J, Cramm J, Litz C, et al. Pilot trial of genetically modified, attenuated *Salmonella* expressing the E. coli cytosine deaminase gene in refractory cancer patients. Cancer Gene Ther. 2003;10:737–44.
17. Toso JF, Gill VJ, Hwu P, Marincola FM, Restifo NP, Schwartzentruber DJ. Phase I study of the intravenous administration of attenuated *Salmonella typhimurium* to patients with metastatic melanoma. J Clin Oncol. 2002;20:142–52.
18. Hayashi K, Zhao M, Yamauchi K, Yamamoto N, Tsuchiya H, Tomita K, et al. Cancer metastasis directly eradicated by targeted therapy with a modified *Salmonella typhimurium*. J Cell Biochem. 2009;106:992–8.
19. Hoffman RM. Tumor-seeking *Salmonella* amino acid auxotrophs. Curr Opin Biotechnol. 2011;22:917–23.
20. Matsumoto Y, Miwa S, Zhang Y, Zhao M, Yano S, Uehara F, et al. Intraperitoneal administration of tumor-targeting *Salmonella typhimurium* A1-R inhibits disseminated human ovarian cancer and extends survival in nude mice. Oncotarget. 2015;6:11369–77.
21. Zhao M, Yang M, Ma H, Li X, Tan X, Li S, et al. Targeted therapy with a *Salmonella typhimurium* leucine-arginine auxotroph cures orthotopic human breast tumors in nude mice. Cancer Res. 2006;66:7647–52.
22. Hoiseth SK, Stocker BAD. Aromatic-dependent *Salmonella typhimurium* are non-virulent and effective as live vaccines. Nature. 1981;291:238–9.
23. Sebastian F, Michael F, Dino K, Manfred R, Denitsa E, Agata B, et al. aroA-deficient *Salmonella enterica* serovar *typhimurium* is more than a metabolically attenuated mutant. Mbio. 2016;7:e01220–16.
24. Miyake K. Innate recognition of lipopolysaccharide by Toll-like receptor 4–MD-2. Trends Microbiol. 2004;12:186.
25. Knirel YA, Valvano MA. Bacterial lipopolysaccharides: structure, chemical synthesis, biogenesis, and interaction with host cells. SpringerWienNewYork: Vienna, Austria and New York, USA, 2011.
26. Raetz CR, Whitfield C. Lipopolysaccharide endotoxins. Annu Rev Biochem. 2002;71:635–700.
27. Ohto U, Fukase K, Miyake K, Shimizu T. Structural basis of species-specific endotoxin sensing by innate immune receptor TLR4/MD-2. Proc Natl Acad Sci USA. 2012;109:7421–6.
28. Hagar JA, Powell DA, Aachoui Y, Ernst RK, Miao EA. Cytoplasmic LPS activates caspase-11: implications in TLR4-independent endotoxic shock. Science. 2013;341:1250–3.
29. Kayagaki N, Wong MT, Stowe IB, Ramani SR, Gonzalez LC, Akashitakamura S, et al. Noncanonical inflammasome activation by intracellular LPS independent of TLR4. Science. 2013;341:1246–9.
30. Nunesalves C. Host response: new LPS receptors discovered. Nat Rev Microbiol. 2014;12:658
31. Teghanemt A, Zhang D, Levis EN, Weiss JP, Gioannini TL. Molecular basis of reduced potency of underacylated endotoxins. J Immunol. 2005;175:4669–76.
32. Rossignol DP, Lynn M. TLR4 antagonists for endotoxemia and beyond. Curr Opin Investig Drugs. 2005;6:496–502.
33. Weidner N, Semple JP, Welch WR, Folkman J. Tumor angiogenesis and metastasis--correlation in invasive breast carcinoma. N Engl J Med. 1991;324:1–8.
34. O'Reilly MS, Boehm T, Shing Y, Fukai N, Vasios G, Lane WS, et al. Endostatin: an endogenous inhibitor of angiogenesis and tumor growth. Cell. 1997;88:273–94.
35. Walia A, Yang JF, Huang YH, Rosenblatt MI, Chang JH, Azar DT. Endostatin's emerging roles in angiogenesis, lymphangiogenesis, disease, and clinical applications. Biochim Biophys Acta. 2015;1850:2422–38.
36. Shichiri M, Hirata Y. Antiangiogenesis signals by endostatin. FASEB J. 2001;15:1044–53.
37. Hanai J, Dhanabal M, Karumanchi SA, Albanese C, Waterman M, Chan B, et al. Endostatin causes G1 arrest of endothelial cells through inhibition of cyclin D1. J Biol Chem. 2002;277:16464–9.
38. Kim YM, Hwang S, Kim YM, Pyun BJ, Kim TY, Lee ST, et al. Endostatin blocks vascular endothelial growth factor-mediated signaling via direct interaction with KDR/Flk-1. J Biol Chem. 2002;277:27872–9.
39. Sudhakar A, Sugimoto H, Yang C, Lively J, Zeisberg M, Kalluri R. Human tumstatin and human endostatin exhibit distinct antiangiogenic activities mediated by alpha v beta 3 and alpha 5 beta 1 integrins. Proc Natl Acad Sci USA. 2003;100:4766–71.
40. Shi H, Huang Y, Zhou H, Song X, Yuan S, Fu Y, et al. Nucleolin is a receptor that mediates antiangiogenic and antitumor activity of endostatin. Blood. 2007;110:2899–906.
41. Kisker O, Becker CM, Prox D, Fannon M, D'Amato R, Flynn E, et al. Continuous administration of endostatin by intraperitoneally implanted osmotic pump improves the efficacy and potency of therapy in a mouse xenograft tumor model. Cancer Res. 2001;61:7669–74.
42. Perletti G, Concari P, Giardini R, Marras E, Piccinini F, Folkman J, et al. Antitumor activity of endostatin against carcinogen-induced rat primary mammary tumors. Cancer Res. 2000;60:1793.
43. Yamaguchi N, Anand-Apte B, Lee M, Sasaki T, Fukai N, Shapiro R, et al. Endostatin inhibits VEGF-induced endothelial cell migration and tumor growth independently of zinc binding. EMBO J. 1999;18:4414–23.
44. Kulke MH, Bergsland EK, Ryan DP, Enzinger PC, Lynch TJ, Zhu AX, et al. Phase II study of recombinant human endostatin in patients with advanced neuroendocrine tumors. J Clin Oncol. 2006;24:3555–61.
45. Xu R, Ma N, Wang F, Ma L, Chen R, Chen R, et al. Results of a randomized and controlled clinical trial evaluating the efficacy and safety of combination therapy with Endostar and S-1 combined with oxaliplatin in advanced gastric cancer. Oncotargets Ther. 2013;6:925–9.
46. Yang L, Wang JW, Sun Y, Zhu YZ, Liu XQ, Li WL, et al. Randomized phase II trial on escalated doses of Rh-endostatin (YH-16) for advanced non-small cell lung cancer. Chin J Oncol. 2006;28:138–41.
47. Jia H, Li Y, Zhao T, Li X, Hu J, Yin D, et al. Antitumor effects of Stat3-siRNA and endostatin combined therapies, delivered by

attenuated *Salmonella*, on orthotopically implanted hepatocarcinoma. Cancer Immunol Immunother. 2012;61:1977–87.
48. Li X, Li Y, Wang B, Ji K, Liang Z, Guo B, et al. Delivery of the co-expression plasmid pEndo-Si-Stat3 by attenuated *Salmonella* serovar typhimurium for prostate cancer treatment. J Cancer Res Clin Oncol. 2013;139:971–80.
49. Li C, Chen X, Kou L, Hu B, Zhu LP, Fan YR, et al. Selenium-*Bifidobacterium longum* as a delivery system of endostatin for inhibition of pathogenic bacteria and selective regression of solid tumor. Exp Ther Med. 2010;1:129–35.
50. Wang S, Kong Q, Curtiss R 3rd. New technologies in developing recombinant attenuated *Salmonella* vaccine vectors. Microb Pathog. 2013;58:17–28.
51. Hitchcock PJ, Brown TM. Morphological heterogeneity among *Salmonella* lipopolysaccharide chemotypes in silver-stained polyacrylamide gels. J Bacteriol. 1983;154:269–77.
52. Kong Q, Yang J, Liu Q, Alamuri P, Roland KL, Curtiss R. Effect of deletion of genes involved in lipopolysaccharide core and O-antigen synthesis on virulence and immunogenicity of *Salmonella enterica* serovar *typhimurium*. Infect Immun. 2011;79:4227.
53. Seung-Hwan P, Hai ZJ, Hong NV, Jiang SN, Dong-Yeon K, Michael S, et al. RGD peptide cell-surface display enhances the targeting and therapeutic efficacy of attenuated *Salmonella*-mediated cancer therapy. Theranostics. 2016;6:1672–82.
54. Porter AG, Jänicke RU. Emerging roles of caspase-3 in apoptosis. Cell Death Differ. 1999;6:99–104.
55. Fina L, Molgaard H, Robertson D, Bradley N, Monaghan P, Delia D, et al. Expression of the *CD34* gene in vascular endothelial cells. Blood. 1990;75:2417–26.
56. Bretscher LE, Morrell MT, Funk AL, Klug CS. Purification and characterization of the L-Ara4N transferase protein ArnT from *Salmonella typhimurium*. Protein Expr Purif. 2006;46:33–9.
57. Herrera CM, Hankins JV, Trent MS. Activation of PmrA inhibits LpxT-dependent phosphorylation of lipid A promoting resistance to antimicrobial peptides. Mol Microbiol. 2010;76:1444–60.
58. Lee H, Hsu FF, Turk J, Groisman EA. The PmrA-regulated gene mediates phosphoethanolamine modification of lipid A and polymyxin resistance in *Salmonella enterica*. Mol Microbiol. 2004;186:4124–33.
59. Stead CM, Pride AC, Trent MS. Genetics and biosynthesis of lipid A. Vienna: Springer; 2011.
60. Raetz CR, Reynolds CM, Trent MS, Bishop RE. Lipid A modification systems in Gram-negative bacteria. Annu Rev Biochem. 2007;76:295–329.
61. Toley BJ, Forbes NS. Motility is critical for effective distribution and accumulation of bacteria in tumor tissue. Integr Biol. 2012;4:165–76.
62. Kasinskas RW, Forbes NS. *Salmonella typhimurium* lacking ribose chemoreceptors localize in tumor quiescence and induce apoptosis. Cancer Res. 2007;67:3201–9.
63. Crull K, Bumann D, Weiss S. Influence of infection route and virulence factors on colonization of solid tumors by *Salmonella enterica* serovar *typhimurium*. FEMS Immunol Med Microbiol. 2011;62:75–83.
64. Leschner S, Westphal K, Dietrich N, Viegas N, Jablonska J, Lyszkiewicz M, et al. Tumor invasion of *Salmonella enterica* serovar *typhimurium* is accompanied by strong hemorrhage promoted by TNF-α. PLoS ONE. 2009;4:e6692.
65. Stritzker J, Weibel S, Seubert C, Götz A, Tresch A, Van RN, et al. Enterobacterial tumor colonization in mice depends on bacterial metabolism and macrophages but is independent of chemotaxis and motility. Int J Med Microbiol. 2010;300:449–56.
66. Zhao M, Yang M, Li XM, Jiang P, Baranov E, Li S, et al. Tumor-targeting bacterial therapy with amino acid auxotrophs of GFP-expressing *Salmonella typhimurium*. Proc Natl Acad Sci USA. 2005;102:755.
67. Zheng JH, Nguyen VH, Jiang SN, Park SH, Tan W, Hong SH, et al. Two-step enhanced cancer immunotherapy with engineered *Salmonella typhimurium* secreting heterologous flagellin. Sci Transl Med. 2017;9:eaak9537.
68. Binder DC, Wainwright DA. The boosting potential of bacteria in cancer immunotherapy. Trends Mol Med. 2017;23:580–2.
69. Kong Q, Six DA, Roland KL, Liu Q, Gu L, Reynolds CM, et al. *Salmonella* synthesizing 1-monophosphorylated LPS exhibits low endotoxic activity while retaining its immunogenicity. J Immunol. 2011;187:412–23.
70. Bravo D, Silva C, Carter JA, Hoare A, Alvarez SA, Blondel CJ, et al. Growth-phase regulation of lipopolysaccharide O-antigen chain length influences serum resistance in serovars of *Salmonella*. J Med Microbiol. 2008;57:938–46.
71. Gunn JS. The *Salmonella* PmrAB regulon: lipopolysaccharide modifications, antimicrobial peptide resistance and more. Trends Microbiol. 2008;16:284–90.
72. Frahm M, Felgner S, Kocijancic D, Rohde M, Hensel M, Roy Curtiss I, et al. Efficiency of conditionally attenuated *Salmonella enterica* serovar *typhimurium* in bacterium-mediated tumor therapy. Mbio. 2015;6:e00254–15.
73. Zhang Y, Cao W, Toneri M, Zhang N, Kiyuna T, Murakami T, et al. Toxicology and efficacy of tumor-targeting *Salmonella typhimurium* A1-R compared to VNP 20009 in a syngeneic mouse tumor model in immunocompetent mice. Oncotarget. 2017;8:54616–28.
74. Arrach N, Cheng P, Zhao M, Santiviago CA, Hoffman RM, Mcclelland M. High-throughput screening for *Salmonella* avirulent mutants that retain targeting of solid tumors. Cancer Res. 2010;70:2165.
75. Yu B, Yang M, Shi L, Yao Y, Jiang Q, Li X, et al. Explicit hypoxia targeting with tumor suppression by creating an "obligate" anaerobic *Salmonella typhimurium* strain. Sci Rep. 2012;2:436.
76. Kocijancic D, Felgner S, Schauer T, Frahm M, Heise U, Zimmermann K, et al. Local application of bacteria improves safety of *Salmonella*-mediated tumor therapy and retains advantages of systemic infection. Oncotarget. 2017;8:49988–50001.
77. Hong EH, Chang SY, Lee BR, Pyun AR, Kim JW, Kweon MN, et al. Intratumoral injection of attenuated *Salmonella* vaccine can induce tumor microenvironmental shift from immune suppressive to immunogenic. Vaccine. 2013;31:1377–84.
78. Zheng JH, Min JJ. Targeted cancer therapy using engineered *Salmonella typhimurium*. Chonnam Med J. 2016;52:173–84.
79. Nguyen VH, Min JJ. *Salmonella*-mediated cancer therapy: roles and potential. Nucl Med Mol Imaging. 2017;51:118–26.
80. Jiang SN, Park SH, Lee HJ, Zheng JH, Kim HS, Bom HS, et al. Engineering of bacteria for the visualization of targeted delivery of a cytolytic anticancer agent. Mol Ther. 2013;21:1985–95.
81. Kim JE, Phan TX, Nguyen VH, Dinhvu HV, Zheng JH, Yun M, et al. *Salmonella typhimurium* suppresses tumor growth via the pro-inflammatory cytokine interleukin-1β. Theranostics. 2015;5:1328–42.
82. Phan TX, Nguyen VH, Duong MT, Hong Y, Choy HE, Min JJ. Activation of inflammasome by attenuated *Salmonella typhimurium* in bacteria-mediated cancer therapy. Microbiol Immunol. 2015;59:664–75.
83. Zhang M, Swofford CA, Forbes NS. Lipid A controls the robustness of intratumoral accumulation of attenuated *Salmonella* in mice. Inter J Cancer. 2014;135:647–57.
84. Clairmont C, Lee KC, Pike J, Ittensohn M, Low KB, Pawelek J, et al. Biodistribution and genetic stability of the novel antitumor agent VNP20009, a genetically modified strain of *Salmonella typhimurium*. J Infect Dis. 2000;181:1996–2002.

85. Luo X, Li Z, Lin S, Le T, Ittensohn M, Bermudes D, et al. Antitumor effect of VNP20009, an attenuated *Salmonella*, in murine tumor models. Oncol Res. 2001;12:501–8.
86. Kelly MG, Alvero AB, Chen R, Silasi DA, Abrahams VM, Chan S, et al. TLR-4 signaling promotes tumor growth and paclitaxel chemoresistance in ovarian cancer. Cancer Res. 2006; 66:3859–68.
87. Kong Q, Six DA, Liu Q, Gu L, Roland KL, Raetz CRH, et al. Palmitoylation state impacts induction of innate and acquired immunity by the *Salmonella enterica* serovar *typhimurium* msbB mutant. Infect Immun. 2011;79:5027–38.
88. Kong Q, Six DA, Liu Q, Gu L, Wang S, Alamuri P, et al. Phosphate groups of lipid A are essential for *Salmonella enterica* serovar *typhimurium* virulence and affect innate and adaptive immunity. Infect Immun. 2012;80:3215–24.
89. Reed SG, Bertholet S, Coler RN, Friede M. New horizons in adjuvants for vaccine development. Trends Immunol. 2009;30: 23–32.
90. Dessel NV, Swofford CA, Forbes NS. Potent and tumor specific: arming bacteria with therapeutic proteins. Ther Deliv. 2015;6:385–99.
91. Liu F, Zhang L, Hoffman RM, Zhao M. Vessel destruction by tumor-targeting *Salmonella typhimurium* A1-R is enhanced by high tumor vascularity. Cell Cycle. 2010;9:4518–24.
92. Hassan JO, Rd CR. Control of colonization by virulent *Salmonella typhimurium* by oral immunization of chickens with avirulent delta cya delta crp *S. typhimurium*. Res Microbiol. 1990;141: 839–50.
93. Roland K, Rd CR, Sizemore D. Construction and evaluation of a delta cya delta crp *Salmonella typhimurium* strain expressing avian pathogenic *Escherichia coli* O78 LPS as a vaccine to prevent airsacculitis in chickens. Avian Dis. 1999;43:429–41.
94. Kang HY, Srinivasan J, Curtiss R. Immune responses to recombinant pneumococcal PspA antigen delivered by live attenuated *Salmonella enterica* serovar *typhimurium* vaccine. Infect Immun. 2002;70:1739–49.